SUPPORTED NANOSTRUCTURED CATALYSTS: METAL COMPLEXES AND METAL CLUSTERS

B. C. Gates

Department of Chemical Engineering and Materials Science, University of California, Davis, California 95616

Many catalysts are nanomaterials dispersed on the surfaces of solid supports, typically nanoporous materials. The simplest and most thoroughly investigated supported catalysts are metal complexes such as $Rh(CO)_2$ *and metal clusters such as* Ir_4*. Metals in the catalysts are covalently bonded to oxygen atoms at the surfaces of metal oxide and zeolite supports; the supports are monodentate or polydentate ligands. When the metals are from Group 7 or Group 8, the metal–oxygen bonding distances are* 2.15 ± 0.10 *Å, essentially the same as*

ADVANCES IN CHEMICAL ENGINEERING, VOL. 27
0065-2377/01 $35.00

in molecular analogues, as shown by extended X-ray absorption fine-structure spectroscopy and density functional theory. The syntheses and patterns of reactivity of supported metal complexes and nanoclusters are consistent with the rules of conventional organometallic chemistry, but site isolation of the supported species stabilizes coordinative unsaturation of the metals and allows for new reactivities and catalytic activities, including those for relatively unreactive compounds such as alkanes. Density functional theory indicates that supported Ir_4 *clusters on zeolite NaX are nearly neutral. The theory also shows that* Os_5C *clusters are bonded much more strongly at surface defect sites than at defect-free sites on MgO. Supported clusters of only a few metal atoms have catalytic properties different from those of larger supported nanoclusters and nanoparticles of metal; they offer intriguing prospects for new catalytic properties.*

I. Introduction: Supported Nanostructures as Catalysts

Catalysts were some of the first nanostructured materials applied in industry, and many of the most important catalysts used today are nanomaterials. These are usually dispersed on the surfaces of supports (carriers), which are often nearly inert platforms for the catalytically active structures. These structures include metal complexes as well as clusters, particles, or layers of metal, metal oxide, or metal sulfide. The solid supports usually incorporate nanopores and a large number of catalytic nanoparticles per unit volume on a high-area internal surface (typically hundreds of square meters per cubic centimeter). A benefit of the high dispersion of a catalyst is that it is used effectively, because a large part of it is at a surface and accessible to reactants. There are other potential benefits of high dispersion as well—nanostructured catalysts have properties different from those of the bulk material, possibly including unique catalytic activities and selectivities.

Besides being small, most catalytic nanomaterials are nonuniform and thus are difficult to characterize well. Consequently, much remains to be learned about them, and chances are excellent that many nanomaterials with novel and useful catalytic properties remain to be discovered.

The goal of this chapter is to illustrate supported catalytic nanomaterials, with an emphasis on those that are simple and well-defined structurally (and thus relatively well understood), and to summarize generally important conclusions about their structure, bonding, reactivity, and catalytic properties. This summary is not exhaustive, and references to related reviews are cited.

Supported catalysts may be classified according to the dimensions of the catalytic components, as follows:

- Mononuclear (single-metal-atom) complexes that are closely analogous to molecular structures
- Multiatom metal, metal oxide, metal sulfide, metal carbide, metal nitride, or metal phosphide nanoclusters that are so small that they have properties different from those of the corresponding bulk materials
- Nanolayers of these materials, the most widely investigated being metal oxides
- Nano- (or larger) particles of these materials that have bulklike properties

This classification includes a distinction between nanoclusters and nanoparticles, although there is still no generally accepted usage distinguishing these terms.

The emphasis here is principally on metals rather than the other materials, because metals are simpler, more widely investigated, and better understood than the others. Supported metal nanoparticles are considered here in only a few summary statements, and nanolayers are beyond the scope of the chapter.

II. Supported Metal Complexes—Molecular Analogues Bonded to Surfaces

The simplest supported catalysts are mononuclear metal complexes, exemplified by industrial supported metallocene catalysts, used (with promoters) for alkene polymerization; these are the so-called single-site catalysts that are finding wide industrial applications (Kristen, 1999; Kaminsky, 1999; Roscoe *et al.,* 1998). The most common supports are metal oxides and zeolites. The metals in these complexes range from oxophilic (e.g., Zr and Ta) to noble (e.g., Rh). Supported metal complexes are stabilized by ligands—in addition to those provided by the support—such as hydride (H), hydrocarbons, and carbonyl (CO). In a typical supported metal complex, the metal is present in a positive oxidation state. Although some such complexes are relatively stable, most are, befitting their roles as catalysts, highly reactive and air- and moisture-sensitive.

In the following paragraphs, methods of preparation and characterization of structurally simple supported metal complexes are summarized, and examples are presented that illustrate characterization data and support general conclusions about structure, bonding, reactivity, and catalysis.

A. PREPARATION

1. Organometallic Chemistry

Many syntheses of supported metal complexes involve simply the reaction of an organometallic precursor in an organic solvent with a support surface; alternatively, a gas-phase precursor may be used in the absence of a solvent. The surface reactions are typically analogous to molecular reactions known from solution organometallic chemistry. The surface chemistry has been reviewed (Lamb, Gates, and Knözinger, 1988; Basset, Lefebvre, and Santini, 1998), and only a few examples are given here.

Deprotonation of a metal hydride precursor may give a surface-bound metal complex and an OH group formed from an oxygen atom on the support surface. For example, $[H_2Os(CO)_4]$ may react with surface oxygen atoms to give surface OH groups and $[HOs(CO)_4]^-$ bonded (ion-paired) to the surface (Lamb, Gates, and Knözinger, 1988). However, the chemistry is often more complex than simple deprotonation and formation of a group (such as an anion) that becomes bonded to the support. This is acid–base chemistry, occurring more readily on a basic surface, such as that of MgO, than on a less basic surface, such as that of SiO_2.

Highly reactive metal complexes with ligands such as alkyls or allyls often react readily with oxygen atoms or OH groups of oxide or zeolite surfaces. For example, $Ta(-CH_2CMe_3)_3(=CHCMe_3)$ (Me is methyl) reacts with surface oxygen atoms of SiO_2 to form mixtures of $\{SiO-\}Ta(-CH_2CMe_3)_2(=CHCMe_3)$ ($\approx$65%) and $\{SiO-\}_2Ta(-CH_2CMe_3)(=CHCMe_3)$ ($\approx$35%) (Vidal *et al.,* 1997). The group denoted in braces, $\{SiO-\}$, represents part of the support—the termination of the bulk solid. $\{SiO-\}$ is a monodentate ligand, and $\{SiO-\}_2$ is a bidentate ligand. In this synthesis, $(-CH_2CMe_3)$ groups are replaced by oxygen atoms of the surface.

In other preparations, oxidative addition of an O–H ligand of an oxide support surface to a metal center of an organometallic complex leads to anchoring of the metal complex to the support (Lamb, Gates, and Knözinger, 1988).

Other synthetic surface reactions are reviewed elsewhere (Lamb, Gates, and Knözinger, 1988; Basset, Lefebvre, and Santini, 1998).

2. Coordination Chemistry

In contrast to the foregoing examples, preparation chemistry on a support surface is often analogous to coordination chemistry in aqueous solutions rather than to organometallic chemistry in organic solutions. Aqueous chemistry is much more typical of the preparation of industrial catalysts than organometallic chemistry, but it is also often much more complex, involving, for example, dissolution of the support and reprecipitation of structures, including mixed-metal species (Che, 2000; Che, Clause, and Marcilly, 1999). Industrial preparation of a supported catalyst often involves a sequence of steps such as the following: contacting of the support with an aqueous solution containing a catalyst precursor such as a metal salt (impregnation), removal of the solvent water, drying, calcination, and possibly reduction and/or sulfidation.

Che (2000) identified a sequence of transformations that are commonly involved during these steps in the preparation of an oxide-supported catalyst in an aqueous environment. First, a hydrated ionic species such as $[PtCl_5(H_2O)]^-$, formed from a precursor metal salt, forms a weakly held outer-sphere complex with the surface of the support, such as γ-Al_2O_3; the interaction may be largely electrostatic, and the chemistry depends on the support and the solution properties, such as the pH. This surface species reacts to form an inner-sphere complex as surface groups (e.g., oxygen atoms) of the support enter the first coordination sphere of the metal (i.e., bond to it); thus, the support acts as a monodentate or polydentate donor ligand. Processes of dissolution–reprecipitation may occur simultaneously with this chemistry, complicating matters; these processes also depend on the solvent chemistry (e.g., the pH). Subsequent treatments, such as calcination, may convert the resultant molecular analogues on the support surface into larger, more complex, and typically nonuniform structures. There are only a few examples of characterization of the intermediates that may be regarded as molecular analogues (Che, 2000).

B. Determination of Composition

Temperature-programmed desorption (or decomposition) with quantitative analysis of gas-phase products (usually by mass spectrometry) has been used to help identify the ligands bonded to a metal in a supported complex. Complications such as reaction of desorbed ligands (e.g., CO) with support groups (e.g., OH) may complicate interpretation of the data (Brenner, 1986).

C. Determination of Metal Oxidation State

Analysis of gas-phase products formed as a precursor reacts with a support surface may provide evidence of the oxidation state of the metal in the resultant supported complex, as illustrated by the following hypothetical stoichiometry of a synthesis on a hydroxylated oxide support (Brenner, 1986):

$$M_1(CO)_j + n\{M_2 - OH\} \rightarrow \{M_2 - O^-\}_n M_1^{n+} + (n/2)H_2 + jCO. \qquad (1)$$

(M_1 and M_2 refer to the metals in the precursor metal carbonyl and in the oxide support, respectively.) Temperature-programmed-oxidation and -reduction experiments provide complementary information.

D. Spectroscopic and Theoretical Characterization of Structure

Spectroscopic methods have been used often to characterize supported metal complexes. Supported metal carbonyls are among the most thoroughly investigated and provide many of the best-understood examples, in part because the CO ligands offer informative fingerprints in the IR spectra, which are easily measured. Metal carbonyl complexes on surfaces are also well suited to characterization by extended X-ray absorption fine-structure (EXAFS) spectroscopy, because the multiple scattering in the linear M–C–O groups allows one to distinguish the C and O backscatterers from other backscatterer ligands bonded to the metal, including those of the support. Supported metal complexes with organic ligands are well suited to characterization by ^{13}C NMR spectroscopy and those with hydride ligands to characterization by ^{1}H NMR spectroscopy. Other useful characterization methods include Raman and ultraviolet/visible spectroscopies.

In recent years researchers have begun to use density functional theory to model supported metal complexes, representing the support as a cluster (fragment of the bulk support). Examples of supported complexes characterized by both theory and spectroscopy are presented below.

When samples incorporate uniform mononuclear metal complexes, then EXAFS data may provide high-quality information about the interactions between the metal and oxygen atoms of the support. Evidence of the metal–support interface has also been determined by theory and, indirectly, by IR spectra indicating the symmetry and thus the number of atoms of the support that act as ligands bonded to the metal.

E. Examples

1. Rhodium Dicarbonyls on Dealuminated Y Zeolite

Rhodium carbonyls on oxide and zeolite supports have been investigated extensively and are some of the best-understood supported metal complexes. These can be formed, for example, from rhodium salts such as $[Rh(NH_3)_5Cl][OH]_2$ (Miessner *et al.,* 1989), from organometallic precursors such as $[Rh(CO)_2(acac)]$ (Goellner, Gates *et al.,* 2000), and even from supported nanoparticles of rhodium metal, which undergo oxidative fragmentation upon treatment with CO when present on hydroxylated surfaces such as that of γ-Al_2O_3 (van't Blik *et al.,* 1985).

A rhodium dicarbonyl formed from $[Rh(NH_3)_5Cl][OH]_2$ (Miessner *et al.,* 1989) or from $[Rh(CO)_2(acac)]$ (Goellner, Gates *et al.,* 2000) on dealuminated Y zeolite has been investigated with IR (Miessner *et al.,* 1989; Goellner, Gates *et al.,* 2000) and EXAFS (Goellner, Gates *et al.,* 2000) spectroscopies and density functional theory (Goellner, Gates *et al.,* 2000) (Fig. 1). The supported complex is represented as $Rh^+(CO)_2$, and the results indicate that it is bonded near an Al atom at a four-ring in the zeolite (Fig. 1). This is an example of a well-defined metal complex on a relatively simple and well-defined (crystalline) support, a faujasite containing only a low density

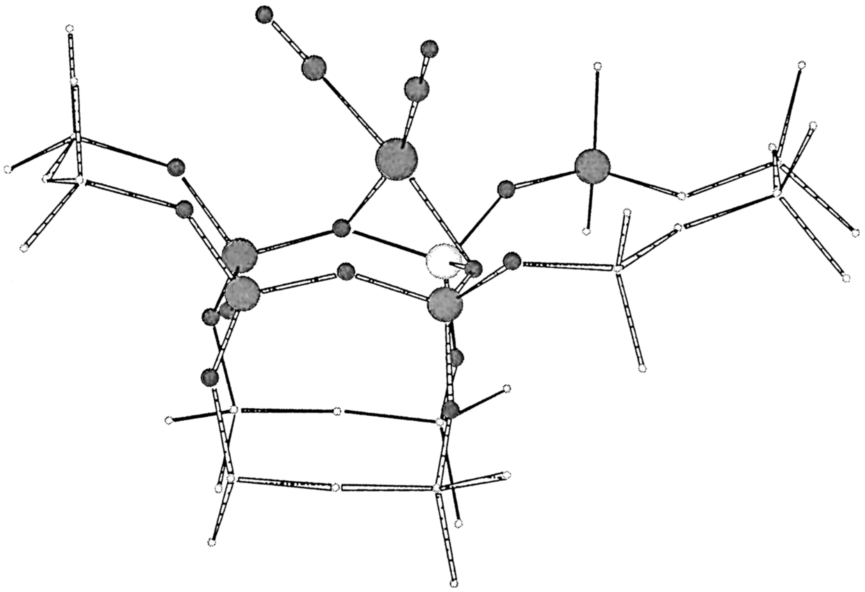

FIG. 1. Model of rhodium dicarbonyl complex on dealuminated Y zeolite, as determined by IR and EXAFS spectroscopies and density functional theory. The Rh atom, near the upper center of the figure, has two CO ligands bonded to it, pointing upward, and two oxygen atoms of the zeolite lattice below. An Al atom is located between these two oxygen atoms. The dangling atoms of the cluster model of the zeolite are capped by hydrogen atoms for the calculation (Goellner, Gates, *et al.,* 2000).

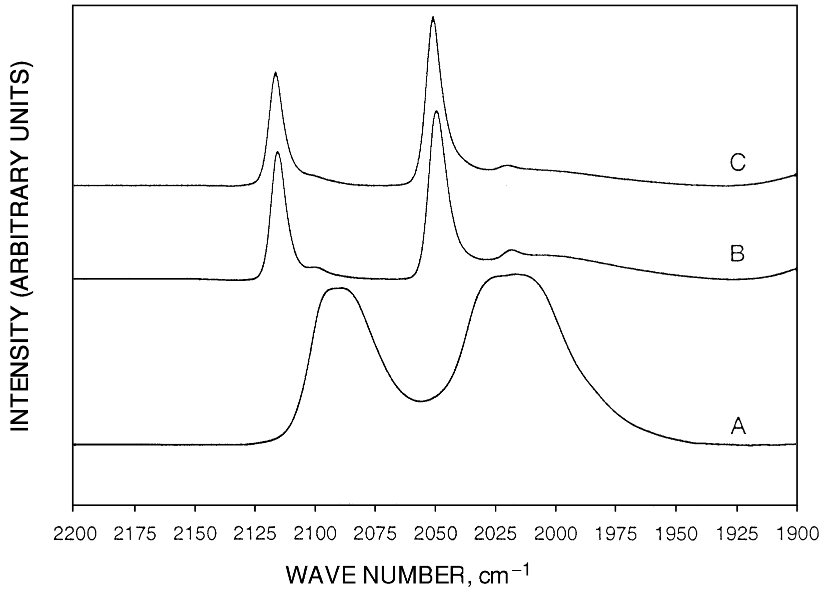

FIG. 2. Infrared spectra in the carbonyl stretching region of Y zeolite-supported $Rh(CO)_2$. (A) Complex in NaY zeolite calcined at 200°C. (B) Complex in dealuminated Y zeolite calcined at 120°C. (C) Complex in dealuminated Y zeolite calcined at 300°C (Goellner, Gates, *et al.,* 2000).

of Al atoms and hence only a low density of bonding sites for the cationic complex. The IR spectra in the carbonyl stretching region (Fig. 2, spectra B and C) are sharp and suggestive of a single species bonded to the support, in contrast to those of $Rh^+(CO)_2$ on a zeolite (NaY) with a higher Al : Si ratio (Fig. 2, spectrum A). The EXAFS spectra and predictions of density functional theory (Table I) agree well with each other and with the IR spectra, being consistent with the structure of Fig. 1. There are two Rh–O bonds in the complex of Fig. 1, and the Rh–O distances are about 2.2 Å (Table I). These are covalent bonding distances, similar to those observed by X-ray diffraction (XRD) crystallography for pure compounds with Rh–O bonds. It is clear that the zeolite support is a bidentate ligand and that the bonds between Rh and O are ordinary covalent bonds.

Miessner (1994) showed that partial decarbonylation of this supported complex by treatment in H_2 at temperatures of 200 to 250°C leads to complexes that are so highly reactive that they combine with N_2 to give well-defined supported complexes with dinitrogen ligands. This remarkable reactivity suggests possibilities for new catalytic properties of these and related supported metal complexes.

TABLE I

COMPARISON OF STRUCTURAL PARAMETERS DETERMINED BY DENSITY FUNCTIONAL THEORY AND BY EXAFS SPECTROSCOPY CHARACTERIZING SAMPLES MADE FROM CHEMISORPTION OF [Rh(CO)$_2$(acac)] ON DEALUMINATED Y ZEOLITE (GOELLNER, GATES *et al.*, 2000)[a]

Calcination temperature (°C) of zeolite support	Calculated			Experimental (EXAFS)				
	Contribution	N	R (Å)	Backscatterer	N	R (Å)	$10^3 \cdot \Delta\sigma^2$(Å^2)	ΔE_0(eV)
300				CO				
	Rh–C	2	1.88	C	2.2	1.86	–0.96	–16.45
	Rh–O*	2	3.03	O*	2.3	2.96	0.49	–7.47
				support				
	Rh–O	2	2.19–2.20	O_{short}	1.9	2.15	0.61	–9.42
	Rh–Al	1	2.80	Al	1.1	2.73	0.88	–17.29
120				CO				
	Rh–C	2	1.88	C	2.3	1.86	–1.33	–17.17
	Rh–O*	2	3.03	O*	2.2	2.97	0.69	–7.80
				support				
	Rh–O	2	2.19–2.20	O_{short}	1.8	2.16	–0.32	–9.30
	Rh–Al	1	2.80	Al	1.3	2.74	0.38	–19.71

[a] Notation: *N*, coordination number; *R*, distance between absorber and backscatterer atom; $\Delta\sigma^2$, Debye–Waller factor; ΔE_0, inner potential correction. Commonly accepted error bounds on structural parameters obtained by EXAFS spectroscopy are N, ±10–15%; R, ±0.02 Å; $\Delta\sigma^2$, ±20%; and ΔE_0, ±20%.

2. *Rhodium Dicarbonyls on γ-Al_2O_3*

Rhodium dicarbonyls on γ-Al_2O_3, similar to those on dealuminated zeolite Y, have been investigated extensively, as summarized by Wovchko and Yates (1999). These complexes, which presumably can be represented as $[\{AlO\}_2Rh(CO)_2]$, can be activated photochemically to remove CO ligands. The resultant surface species react with N_2 in chemistry similar to that mentioned previously for the zeolite-supported analogue; they also react with methane, leading to formation of methyl ligands, which undergo insertion reactions with CO ligands (Wovchko and Yates, 1999). The results suggest possibilities for new catalysts for alkane conversion.

3. *Rhenium Tricarbonyls on MgO*

The analogy between molecular and supported metal complexes is strongly reinforced by results representing rhenium tricarbonyls on MgO. These are some of the most thoroughly investigated samples in this category, having been characterized with many experimental methods as well as density functional theory. The complexes were made on MgO powder from various organometallic precursors, $[HRe(CO)_5]$, $[DRe(CO)_5]$, $[Re_2(CO)_{10}]$, and $[H_3Re_3(CO)_{12}]$ (Kirlin *et al.,* 1990a, 1990b; Triantafillou, Purnell *et al.,* 1994); they have also been made on ultrathin MgO films exposing the (111) face (Purnell *et al.,* 1994a,b). The experimental methods used to investigate the samples were temperature-programmed decomposition and reduction (which confirm the composition) and IR, EXAFS, Raman, ultraviolet-visible, and inelastic electron tunneling spectroscopies (Kirlin, De Thomas *et al.,* 1986; Triantafillou, Purnell *et al.,* 1994). The EXAFS data indicate approximately three CO ligands per Re atom and approximately three support oxygen atoms neighboring each Re atom, consistent with the vibrational spectra and the other data (Papile and Gates, 1992).

Rhenium carbonyls have been prepared on MgO powder with various degrees of hydroxylation (and methoxylation), and IR and EXAFS spectra indicate symmetries of the complexes, e.g., C_{3v} on dehydroxylated MgO; this complex is represented as $Re(CO)_3\{OMg\}_3$ (Papile and Gates, 1992). The IR data show substantial shifts in the ν_{co} bands with changes in the degree of hydroxylation or methoxylation of the MgO surface (Table II), even providing a basis for determining the number of O versus OH ligands from the support that are bonded to a Re atom.

Two limiting-case surface structures, $Re(CO)_3\{OMg\}_3$ and $Re(CO)_3\{HOMg\}_3$, represented here as structures A and B, have been modeled with density functional theory, with the MgO being represented as a fragment of its surface, shown in the structures below (Hu *et al.,* 1999). Consistent with the experimental results, the most stable species (structure A) was found to exist

TABLE II

SUMMARY OF STRUCTURAL ASSIGNMENTS AND IR SPECTRA OF RHENIUM TRICARBONYLS ON MgO (PAPILE AND GATES, 1992)

Structural model	Precursor	MgO pretreatment temperature,°C	Symmetry indicated by IR spectrum	v, frequency of high-frequency carbonyl band, cm^{-1}	Δv,[a] cm^{-1}	$\Delta v/(\Delta v)_{\max}$	$N_{O^{2-}}/(N_{O^{2-}} + N_{OH^-})$[b]
$Re(CO)_3\{OMg\}_3$	$[Re_2(CO)_{10}]$	700	C_{3v}	2036	22	1.00	1.00
$Re(CO)_3\{OMg\}_2\{HOMg\}$	$[H_3Re_3(CO)_{12}]$	700	C_s	2028	14	0.64	0.67
$Re(CO)_3\{OMg\}\{HOMg\}_2$	$[Re_2(CO)_{10}]$	400	C_s	2022	8	0.36	0.33
$Re(CO)_3\{HOMg\}_3$	$[Re_2(CO)_{10}]$	390	C_{3v}	2014	0	0.00	0.00

[a] Change in frequency of CO vibration relative to that of $Re(CO)_3\{HOMg\}_3$.

[b] Fraction of groups on MgO surface estimated to be oxygen atoms rather than OH groups.

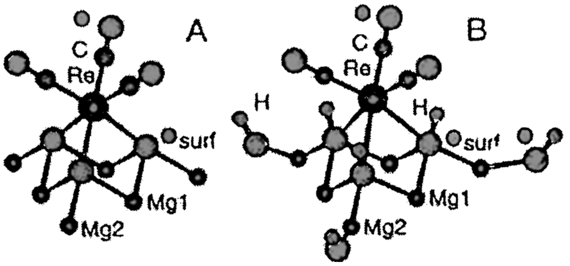

at Mg cation vacancies (corner sites) at the MgO surface. The calculated results agree very well with the symmetry indicated by the IR and EXAFS data; the predictions of the carbonyl stretching frequencies are also in good agreement with experiment (Table III). The theoretical results show that the Re–O bond energy in the dehydroxylated sample (3.5 eV) is greater than the Re–CO bond energy (2.4–2.5 eV), which reinforces the view of the support as a strongly bound tridentate ligand (Table III). The theoretical results (Hu *et al.,* 1999) indicate that the Re–O_{support} distance in $Re(CO)_3\{OMg\}_3$ is 2.15 Å, which is the same as the EXAFS value observed for rhenium carbonyls on MgO powders with few surface OH groups (Triantafillou, Purnell *et al.,* 1994), approximated as $Re(CO)_3\{OMg\}_2\{HOMg\}$. The results imply that the most stable of the surface species, $Re(CO)_3\{OMg\}_3$, is formed preferentially, for example, over $Re(CO)_3\{HOMg\}_3$ or $Re(CO)_3\{OMg\}_2\{HOMg\}$, on slightly hydroxylated MgO surfaces.

TABLE III

Calculated Bond Distances *r*, Binding Energy to the Support Surface, E_b, and Frequencies of $Re(CO)_3$/MgO Bonded to MgO at Various Assumed Defect Sites: Comparison of Predictions of Density Functional Theory (Hu *et al.,* 1999) and Experimental Results (Triantafillou *et al.,* 1994)[a]

Sample	r(Re–O)	r(Re–C)	r(C–O)	E_b	ν(Re–MgO)	ν(Re–CO)	$\Delta\nu$(C–O)[b]
$Re(CO)_3\{OMg\}_3$							
Theory							
$Re(0)(CO)_3/V_s^{-c}$	2.26	1.90	1.18	2.79	528	510	−153
$Re(I)(CO)_3/V_s^{-c}$	2.15	1.95	1.16	3.51	552	479	−93
$Re(I)(CO)_3/V_s^{c}$	2.05	2.02	1.15	2.74	551	439	−29
Experiment[d]	2.15	1.88					−107

[a] Distances r in Å, binding energy E_b of $Re(CO)_3$ species to MgO in eV per Re–O bond (three bonds), vibrational frequencies ν in cm^{-1}.

[b] Frequency shift with respect to free CO: experiment, 2143 cm^{-1}; calculation, 2120 cm^{-1}.

[c] Notation: Re(0) is zerovalent rhenium, Re(I) is Re^+. V_s refers to a cation defect site; removal of Mg^+ from the lattice gives V_s^-, for example.

[d] Further details given elsewhere (Triantafillou *et al.,* 1994).

In summary, the theoretical results representing the rhenium carbonyls on MgO are in very good agreement with the symmetry indicated by the vibrational spectra and with the coordination numbers and bond distances indicated by EXAFS spectroscopy. Thus, the rhenium carbonyls are regarded as prototype supported metal complexes. They reaffirm the strong analogy between surface-bound metal complexes and molecular metal complexes. The MgO surface is clearly identified as a polydentate ligand.

4. *Osmium Di- and Tricarbonyls on* γ*-*Al_2O_3

IR and EXAFS data representing osmium carbonyls on γ-Al_2O_3 led to the identification of osmium di- and tricarbonyls and of the conversion of the latter into the former. The loss of one CO ligand from the tricarbonyl complex (indicated by infrared spectroscopy and confirmed approximately by EXAFS spectroscopy) was accompanied by an increase in the Os–O coordination number from 2.9 to 3.9 (or nearly from 3 to 4) (Deutsch, Chang, and Gates, 1993), as follows:

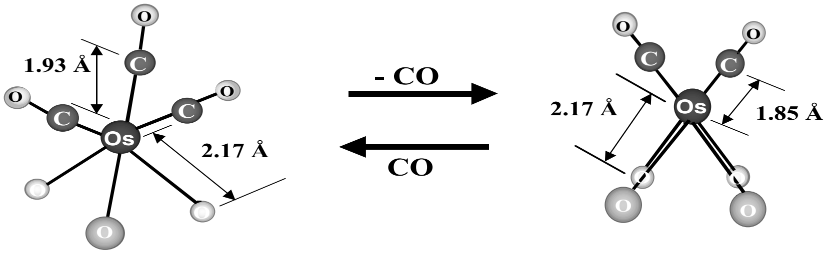

(The bond distances were determined by EXAFS spectroscopy (Deutsch, Chang, and Gates, 1993).) Thus, one CO ligand was replaced by one O ligand of the support surface, and both supported complexes were coordinatively saturated (18-electron) complexes (with O of the surface regarded formally as a two-electron donor). The Os–O, Os–C, and Os–O* distances (O* is carbonyl oxygen) are nearly equal to those of other supported Group 7 and Group 8 metal carbonyls and their molecular analogues.

These results strengthen the analogy between molecular and supported metal carbonyl complexes and extend it beyond structure and bonding to reactivity.

Osmium carbonyls on MgO and on γ-Al_2O_3, among other oxides, are catalysts (or catalyst precursors) for alkene isomerization and hydrogenation (Li *et al.,* 1984). The activity depends on the metal oxide used as a support. The ligands present on the metal during catalysis have not yet been elucidated.

5. *Tantalum Hydride Complexes on SiO_2*

When the SiO_2-supported tantalum complexes mentioned previously were treated with H_2, a surface tantalum hydride formed, $HTa\{OSi\}_2$. This catalyzes propane metathesis, giving equimolar mixtures of ethane and butane (Vidal *et al.,* 1997). This is a new reaction, clear evidence of new catalytic properties associated with a highly reactive surface-bound metal complex. In this example—and the examples involving rhodium complexes reacting with N_2 and with CH_4, for example—it is important that the rather rigid polydentate ligand provided by the support surface stabilizes the metals with degrees of coordinative unsaturation that readily allow bonding of even relatively unreactive compounds—and sometimes subsequent catalytic conversion. This is an advantage of site isolation of the metal complex; analogous metal complexes in solution do not easily retain coordinative unsaturation because they react with each other.

F. Generalizations about Structure and Bonding

The results summarized here support the following generalizations about structure and bonding of metal complexes bonded to metal oxide and zeolite supports:

- The metal–oxygen distances in metal oxide–supported complexes of Group 7 and Group 8 metals are 2.15 ± 0.10 Å.
- These distances are essentially the same as the metal–oxygen distances determined by XRD crystallography for complexes of the same metals containing electron donor oxygen ligands.
- Metal oxide and zeolite supports are ligands (sometimes monodentate and sometimes polydentate), and the metals are covalently bonded to the oxygen atoms of the support surface.
- The results of density functional theory (for supported rhodium carbonyls and rhenium carbonyls) match the available EXAFS and infrared data well.
- Most reports of supported metal complexes lack evidence of the support ligands, but we may infer that they are usually oxygen atoms or OH groups of the surface when the support is a metal oxide or a zeolite.

G. Generalizations about Reactivity and Catalysis

- The patterns of reactivity typically mimic those of analogous metal complexes in solution; the rules of organometallic chemistry apply.

- However, the fact that the supported metal complexes are site-isolated (and unable to react with each other) opens up possibilities for stabilization of coordinative unsaturation of the metals and new reactivities.
- Some supported metal complexes have new catalytic properties, and new supported metal complexes with unexpected catalytic properties seem likely to be discovered.

III. Metal Pair Sites and Triplet Sites on Supports

The metal complexes described previously, except for those supported on the dealuminated zeolite, were bonded to intrinsically heterogeneous surfaces, and the bonding sites have not been determined precisely. To a first approximation, the metal complexes on some supports (e.g., SiO_2 or γ-Al_2O_3) might be assumed to be almost randomly distributed over the surfaces, but on other supports (e.g., MgO), this seems less likely. Much remains to be learned about the specific sites on the supports where the complexes form, specifically, whether these are defect sites.

An obvious question is whether patterned arrays of metal complexes can be formed on supports, and an approach to the preparation of such materials has been made by use of precursors containing more than one metal atom. Thus, attempts have been made to prepare supported metals with pair (and triplet) sites from dimeric (and trimeric) complexes of oxophilic metals, including Mo, W, and Re, which bond strongly to oxide surfaces.

EXAFS data characterizing SiO_2-supported molybdenum species made from $[Mo_2(allyl)_4]$ have led to precise structural models, including those of surface dimers (with Mo–Mo bonds) and pair sites (without Mo–Mo bonds) (Iwasawa, 1987), but the structures seem to be sensitive to undefined chemistry of the SiO_2 support surfaces and could be difficult to reproduce. Catalytic data for ethylene hydrogenation and butadiene hydrogenation with these samples and with samples expected to have isolated Mo sites point to a catalytic role of the neighboring sites (Iwasawa, 1987).

SiO_2-supported tungsten species prepared from the dimer $[Cp_2W_2(CO)_4]$ are characterized by EXAFS data indicating a W–W contribution at a distance of 2.96 Å (too long for a W–W bond); the W–W contribution was found to be small, and stronger evidence of the presence of tungsten pair sites on the support surface is provided by reaction data for the McMurry-type reductive coupling of acetaldehyde or acetone, which was observed in the presence of the sample made from the dimeric precursor but not in the presence of a sample made similarly from a monomeric precursor (Sullivan *et al.,* 1995).

A family of catalysts was made from the aforementioned rhenium carbonyl precursors on MgO, including [$HRe(CO)_5$], [$Re_2(CO)_{10}$], and [$H_3Re_3(CO)_{12}$] (Kirlin, Knözinger, and Gates, 1990; Kirlin, van Zon *et al.,* 1990; Triantafillou *et al.,* 1994). EXAFS data characterizing the samples made from [$H_3Re_3(CO)_{12}$] indicate Re–Re contributions at an average (nonbonding) distance of 3.94 Å (Kirlin, van Zon, *et al.,* 1990). The catalyst made from [$HRe(CO)_5$] was found to lack such contributions and to be catalytically active for propene hydrogenation but not cyclopropane hydrogenolysis, whereas the catalyst prepared similarly from [$H_3Re_3(CO)_{12}$] is catalytically active for both reactions, as are supported nanoparticles of metallic rhenium (Kirlin and Gates, 1987; Kirlin, van Zon, *et al.,* 1990). This comparison suggests that the catalyst made from the mononuclear precursor had isolated rhenium centers, whereas the catalyst made from the trinuclear precursor had neighboring rhenium centers (perhaps groups of three) that constitute the catalytic sites for cyclopropane hydrogenolysis.

These results seem to offer a foretaste of possibilities for tailoring multicenter catalytic sites on support surfaces, but this field is still in its infancy.

IV. Supported Metal Nanoclusters

The importance of supported metal nanoclusters and nanoparticles in catalysis and the rough analogy between supported nanoclusters and organometallic cluster compounds (those with metal–metal bonds) in catalysis have motivated researchers to find connections between these two classes of materials. Thus, an obvious synthetic goal has been size-selected metal nanoclusters on supports.

Supported metal nanoclusters differ from the supported metal complexes discussed in the earlier part of this chapter by having more than one metal atom and metal–metal bonds; they may or may not have stabilizing ligands in addition to the support, and when they lack such ligands they have coordinative unsaturation and can bond to reactive ligands and be catalytically active. Part of the motivation for attempting to prepare uniform (size-selected) nanoclusters is related to the sometimes dramatic changes in properties of materials that result as the size decreases from bulk to molecular (nanocluster) dimensions. Thus, one thinks of tuning the catalytic properties of these clusters by size selection.

This section of this chapter includes a brief review of methods of preparation and properties of supported metal nanoclusters; only catalysts that have been relatively well characterized and found to be nearly uniform are considered. The nanoclusters described here lack the structural definition of organometallic cluster compounds such as metal carbonyl clusters (e.g., $[Rh_6(CO)_{16}]$), and, by and large, they are not as well defined structurally as the simpler supported mononuclear metal complexes described here. The supported clusters described here differ from bare metal nanoclusters in the gas phase, because the supports provide ligands. Nonetheless, supported nanoclusters may be coordinatively unsaturated by virtue of their stable isolation, so that reactants can bond to them.

A. PREPARATION

In attempts to prepare uniform supported clusters on well-defined planar supports, physicists have relied on impingement of beams of size-selected gas-phase clusters (Meiwes-Broer, 2000; Heiz *et al.,* 1999; Heiz and Schneider, 2000). This method has become quite popular, with work now underway in a number of laboratories, and it offers the advantage that, in prospect, it can be used with any metal of any cluster size. Limitations are the restriction to (nearly) planar supports (because of the preparation method) and the uncertainty of the cluster size distributions after deposition. Heiz and colleagues (1999) asserted that “soft landings” of clusters on a support lead to uniform site-isolated clusters, but recent scanning tunneling microscopy images of Si clusters on Ag(111) (Messerli *et al.,* 2000) indicate that some migration and aggregation (sintering) of the clusters is to be expected, at least under some conditions.

An alternative to this physical method of preparing structurally uniform metal clusters on supports involves chemistry by which molecular metal carbonyl clusters (e.g., $[Rh_6(CO)_{16}]$) serve as precursors on the support. These precursors are decarbonylated with maintenance of the metal frame to give supported nanoclusters (e.g., Rh_6). Advantages of this chemical preparation method are its applicability to many porous supports, such as zeolites (and not just planar surfaces) and the opportunities to use spectroscopic methods to follow the chemistry of synthesis of the precursor on the support and its subsequent decarbonylation. Zeolites, because their molecular-scale cages are part of a regular (crystalline) structure, offer the prospect of regular three-dimensional arrays of nanoclusters.

A limitation of supported metal nanoclusters prepared from molecular metal carbonyl clusters is that, so far, clusters of only several metals (Ru, Rh, Ir, and Os) have been made in high yields (80 to 90%, with the likely impurity species being mononuclear metal complexes). However, this disadvantage is offset by the advantage of the characterizations, which show that some clusters are stable even during catalysis, at least under mild conditions.

Supported nanoclusters made from metal carbonyl clusters are emphasized here, because there are numerous characterization data on which to base the discussion. The synthetic methods are illustrated by the following examples.

Molecularly or ionically dispersed metal carbonyl clusters on metal oxides have been prepared in high yields by reaction of metal carbonyl clusters with support surfaces or by syntheses on support surfaces from mononuclear precursors (Gates and Lamb, 1989; Iwasawa, 1993; Ichikawa, 1992; Gates, 1994). Synthesis of supported metal carbonyl clusters has been reviewed recently (Gates, 1995, 1998), and only a few examples are included here.

A simple reaction involves a metal carbonyl cluster and surface OH groups. For example, $[Ir_4(CO)_{12}]$ reacts with OH groups of MgO, giving adsorbed $[HIr_4(CO)_{11}]^- + HCO_3{}^-$. The adsorbed $[HIr_4(CO)_{11}]^-$ is converted into $[Ir_6(CO)_{15}]^{2-}$ by treatment in CO (Zhao and Gates, 1997).

Another class of synthesis reaction is deprotonation of a hydrido metal carbonyl cluster on a basic surface. For example, $[H_4Os_4(CO)_{12}]$ reacts with MgO or with γ-Al_2O_3 to give $[H_3Os_4(CO)_{12}]^-$, which is part of a surface ion pair on the support (Budge, Scott, and Gates, 1983).

Some metal carbonyl clusters can be prepared efficiently on surfaces from mononuclear metal carbonyl precursors, e.g., $[Rh(CO)_2(acac)]$, $[Ir(CO)_2(acac)]$, and $[Pt(allyl)_2]$. The chemistry occurring on γ-Al_2O_3 illustrates the subtlety of the syntheses and the analogy to solution chemistry. Depending on the basicity of the γ-Al_2O_3 surface, which is regulated by the temperature of treatment to control the degree of dehydroxylation of the initially hydroxylated γ-Al_2O_3, the surface species formed by carbonylation of the adsorbed species formed from $[Ir(CO)_2(acac)]$ may be predominantly any of the following: $[Ir_4(CO)_{12}]$, $[HIr_4(CO)_{11}]^-$, $[Ir_8(CO)_{22}]^{2-}$, or $[Ir_6(CO)_{15}]^{2-}$ (Zhao and Gates, 1997).

In all these syntheses, the surface chemistry is analogous to known solution chemistry (Gates, 1994). Thus, syntheses on nearly neutral surfaces, for example, that of $[Ir_4(CO)_{12}]$ on γ-Al_2O_3 (Kawi, Chang, and Gates, 1993) and that of $[H_4Ru_4(CO)_{12}]$ and of $[H_4Os_4(CO)_{12}]$ on SiO_2 (Dossi *et al.,* 1990), take place as in neutral solvents. The syntheses on the basic surface of MgO take place as in basic solutions. Roberto and colleagues (1996) made SiO_2 surfaces basic by incorporation of alkali metal carbonates and tuned the basicity and thus the reactivity by varying the type and amount of the carbonate.

Sometimes solution reactions take place in the presence of reducing agents, and evidently the reducing sites on MgO play an analogous role (Lamb, Gates, and Knözinger, 1988). The reactivities of all the metal oxides are influenced by the treatment conditions and methods of preparation, which influence, for example, the degree of hydroxylation and the base strength of the surface.

The syntheses that take place on metal oxide surfaces also take place in zeolite cages. Reactions in the nearly neutral zeolite NaY are similar to those occurring on some γ-Al_2O_3 surfaces, and those in basic zeolite NaX resemble those on basic metal oxide surfaces, such as that of hydroxylated MgO. "Ship-in-a-bottle" syntheses take place when clusters formed in zeolite cages are trapped there because they are too large to fit through the apertures connecting the cages (Kawi and Gates, 1994).

Supported nanoclusters have been prepared by decarbonylation of neutral or anionic metal carbonyl clusters on supports. The decarbonylation chemistry is not fully understood. The chemistry accompanying removal of the CO ligands from metal carbonyl clusters on metal oxides evidently involves hydroxyl groups or water on the surface of the metal oxide.

For example, the decarbonylation of $[Ir_4(CO)_{12}]$ on γ-Al_2O_3 in He at 473 K takes place with little or no disruption of the tetrahedral Ir_4 frame (Kawi, Chang, and Gates, 1993). Decarbonylation of MgO-supported $[HIr_4(CO)_{11}]^-$ and of $[Ir_6(CO)_{15}]^{2-}$ takes place with near retention of the respective tetrahedral and octahedral metal frames in He at 573 K (van Zon *et al.,* 1993). However, decarbonylation of tetrairidium carbonyl clusters formed from $[Ir_4(CO)_{12}]$ on highly hydroxylated MgO takes place with sintering of the iridium to give larger, nonuniform nanoclusters or particles (Triantafillou and Gates, 1994). Sintering is affected in a complex way by surface OH groups, and generalizations about the effects of these groups seem not yet to be warranted.

B. STRUCTURAL CHARACTERIZATION

The methods of structure determination of supported nanoclusters are essentially the same as those mentioned previously for supported metal complexes. EXAFS spectroscopy plays a more dominant role for the metal clusters than for the complexes because it provides good evidence of metal–metal bonds. Combined with density functional theory, EXAFS spectroscopy has provided much of the structural foundation for investigation of supported metal clusters. EXAFS spectroscopy provides accurate determinations of metal–metal distances (±1–2%), but it gives only average structural information and relatively imprecise values of coordination numbers. EXAFS spectroscopy provides structure data that are most precise when the clusters are extremely small (containing about six or fewer atoms) and nearly uniform (Alexeev and Gates, 2000).

C. EXAMPLES

$[Rh_6(CO)_{16}]$ was prepared on the surface of TiO_2 powder by adsorption of $[Rh(CO)_2(acac)]$ followed by treatment in CO. IR and EXAFS data indicate the presence of $[Rh_6(CO)_{16}]$ (Goellner and Gates, 2001). The decarbonylated sample is well approximated as Rh_6 on TiO_2, as shown by the EXAFS result indicating a Rh–Rh first-shell coordination number of about 4, the value for an octahedral metal frame (as in $[Rh_6(CO)_{16}]$) (Goellner and Gates, 2001).

Similar results have been obtained for $[Ir_4(CO)_{12}]$ (and Ir_4 formed from it) on various supports and for $[Ir_6(CO)_{16}]$ (and Ir_6 formed from it) on various supports; details are given elsewhere (Gates, 1998). One of the most thoroughly investigated supported clusters is Ir_4 in zeolite NaX, which has been characterized by EXAFS spectroscopy and density functional theory (Ferrari *et al.,* 1999). The EXAFS data indicate an Ir–Ir coordination number of nearly 3, as expected for an Ir_4 tetrahedron, and the theory confirms the stability of Ir_4 tetrahedra assumed to be placed at six-rings in the faujasite zeolite (Fig. 3). EXAFS spectroscopy also characterizes the metal–support interface in terms of M–O coordination numbers and distances (although the uncertainty in the parameters is markedly greater than for first-shell metal–metal contributions). Both relatively short metal–support oxygen ($M–O_s$) distances of about 2.1–2.2 Å and relatively long $M–O_l$ distances of about 2.5–2.7 Å are typical EXAFS results for the metal–support interface (Koningsberger and Gates, 1992), being determined with precisions of 1 to 2%. The $M–O_s$ coordination numbers are much less precise than the distances and do not lead to strong generalizations, except that an $M–O_s$ coordination number of roughly 1 to 2 is typical of noble metal nanoclusters on

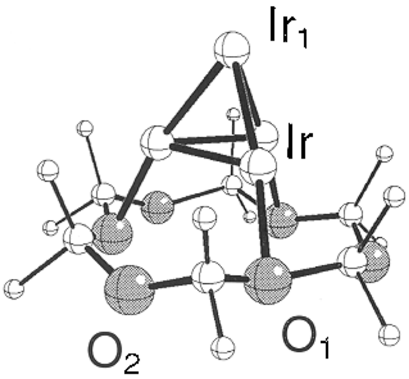

FIG. 3. Model of Ir_4 bonded at a six-ring in zeolite NaX with an Al : Si ratio of 1, as modeled by density functional theory (Ferrari *et al.,* 1999).

oxide and zeolite supports. (The quality of the EXAFS data characterizing the metal–support interactions in supported metal clusters is generally not as good as that characterizing the metal–support interactions in supported metal complexes, because the metal–support contributions are greater for the latter samples; the metal–metal contributions dominate for supported metal clusters.)

The theoretical parameters characterizing Ir_4 in zeolite NaX (Fig. 3) indicate Ir–O distances of about 2.2 Å, in good agreement with EXAFS data (Ferrari *et al.,* 1999) and approximately equal to the metal–oxygen bond distances found experimentally and theoretically for supported metal complexes, as discussed above. When the structure of Fig. 3 is rotated 60°, the theory indicates an Ir–O distance of about 2.7 Å, in agreement with the longer distances observed by EXAFS spectroscopy (but this agreement may be fortuitous).

Similarly, theoretical results for Os_5C on MgO (Fig. 4), prepared from $[Os_5C(CO)_{14}]^{2-}$, are in good agreement with EXAFS data characterizing the metal frame, and they indicate $Os{-}O_s$ distances of about 2.1 Å, about the same as the values mentioned above and in good agreement with the EXAFS data. The bond distances suggest that the oxygen of the support serves as a ligand to a supported metal cluster, much as it serves as a ligand to a supported metal complex.

FIG. 4. Models of Os_5C on the (100) face of MgO, as modeled by density functional theory (Goellner, Neyman, *et al.,* 2000). The structure at the right is represented on the defect-free surface, and the structure at the left is represented at a cation defect site of the surface. The binding energy of the Os_5C cluster to the fragment of MgO in the structure shown at the left (where an Mg cation is missing) was calculated to be 4.89 eV, and the binding energy of the Os_5C cluster to the defect-free MgO fragment shown at the right was calculated to be 0.59 eV; thus, the former structure is much more tightly bound than the former.

When the structure at the right in Fig. 4 is rotated 90°, the distance indicated by theory is about 2.6 Å, again in good agreement with EXAFS data for the longer Os–O_l distance (Panjabi, 2000; Koningsberger and Gates, 1992) (but this agreement may be fortuitous).

The theoretical metal–metal distances in both the supported Ir_4 and Os_5C clusters are significantly (about 0.2 Å) less than the metal–metal distances determined by EXAFS spectroscopy; the most likely explanation of this difference (confirmed by theory) is that some residual ligands, such as carbon, remained on the metal frames after decarbonylation (Ferrari *et al.,* 1999; Goellner, Neyman *et al.,* 2000). Recent EXAFS results for Rh_6 on TiO_2 (Goellner and Gates, 2001) are consistent with the presence of carbon on some decarbonylated clusters—but not on others, depending on the preparation conditions.

The theoretical investigations of supported nanoclusters provide additional insights about the role of the support. Theory indicates that Ir_4 clusters on zeolite NaX are neutral or slightly negatively charged and that cluster–support bonding induces a polarization of the cluster that could affect reactivity and catalysis (Ferrari *et al.,* 1999). The theoretical investigation of supported Os_5C clusters provides evidence that the clusters on the defect-free (001) face of MgO (Fig. 4) are much less strongly bound than the clusters at cation vacancy sites, which are common on MgO; the clusters are tightly bound at the defect sites (Goellner, Neyman *et al.,* 2000). The result is suggested to be valid with some generality for nanoclusters on oxide supports; this suggestion is important for its implications regarding the stability of supported nanoclusters, for example, during catalysis.

D. CATALYTIC PROPERTIES

EXAFS spectra representing catalyst–support combinations, $Ir_4/\gamma\text{-}Al_2O_3$, $Ir_6/\gamma\text{-}Al_2O_3$, and Ir_4/MgO, show that the cluster frames were maintained before, during (Table IV), and after catalysis of propene hydrogenation, provided that the conditions were mild (e.g., room temperature and 1 atm) (Panjabi, Argo, and Gates, 1999), but when the temperature of catalysis reached about 150°C, the metals aggregated on the support. The data suggest that the supported clusters themselves are catalytically active. The ligands on the clusters during catalysis are not yet fully determined, and it is possible that residual ligands (such as C) remaining from the CO of the precursor clusters were present in addition to hydrocarbon and hydrogen observed by IR spectroscopy.

The rates of toluene hydrogenation catalyzed by Ir_4 and by Ir_6 supported on metal oxides and zeolites differ from each other, typically by factors of

TABLE IV

EXAFS RESULTS CHARACTERIZING SUPPORTED METAL CLUSTERS DURING CATALYTIC HYDROGENATION OF PROPENE FED IN AN EQUIMOLAR MIXTURE TO A FLOW REACTOR OPERATED AT STEADY STATE AT 25°C AND 1 ATM (PANJABI, ARGO, AND GATES, 1999)[a]

Catalyst	EXAFS parameters				
Metal cluster/ support	Shell	N	R(Å)	$10^3 \cdot \Delta\sigma^2$(Å^2)	ΔE_0(eV)
Ir_4/γ-Al_2O_3	Ir–Ir	3.2	2.71	2.4	–3.2
	Ir–$O_{support}$				
	Ir–O_s	1.3	2.17	3.5	–15.6
	Ir–O_l	0.5	2.70	–6.8	–10.9
	Ir–Al	0.3	1.77	9.3	2.6
Ir_6/γ-Al_2O_3	Ir–Ir	4.0	2.71	–5.3	–3.2
	Ir–$O_{support}$				
	Ir–O_s	1.3	2.23	1.2	–18.3
	Ir–O_l	0.5	2.72	5.2	–13.0
	Ir–Al	0.1	1.51	0.6	–3.7
Ir_4/MgO	Ir–Ir	3.0	2.72	1.5	–2.5
	Ir–$O_{support}$				
	Ir–O_s	1.3	2.15	2.0	–12.7
	Ir–O_l	0.5	2.69	–6.3	–9.9

[a] Notation: *N,* coordination number; *R,* distance between absorber and backscatterer atom; $\Delta\sigma^2$, Debye–Waller factor; ΔE_0, inner potential correction; $O^* =$ carbonyl oxygen; the subscripts *s* and *l* refer to short and long, respectively.

several; thus, these supports are roughly equivalent, possibly because they all offer similar ligands to the metal cluster (Gates, 1998).

In prospect, structurally well-defined supported metal clusters provide the opportunity for resolving support from cluster-size effects. A family of supported Ir clusters and particles was prepared from $[Ir_4(CO)_{12}]$ on γ-Al_2O_3 (Xiao *et al.,* 1996). The smallest clusters were approximately Ir_4, and samples with larger nanoclusters and particles were prepared by treating Ir_4/γ-Al_2O_3 in H_2 under various conditions to cause aggregation and vary the average cluster or particle size. The catalytic activity was measured for each sample. The rate per exposed Ir atom increased by two orders of magnitude as the cluster or particle size increased, becoming independent of particle size when the average particle contained about 100 atoms (Xiao *et al.,* 1996). The data for the larger particles conform to the expected pattern for the structure-insensitive reaction, but those for the smaller clusters and particles do not. (A structure-insensitive reaction is one that takes place at approximately the same rate per exposed metal atom, independent of the face of the metal crystal that is exposed or the average size of the metal nanoparticle in the catalyst (Boudart and Djéga-Mariadassou, 1984)).

The cluster-size dependence has not yet been explained; it may reflect an intrinsically low activity of the clusters, but it might also be a consequence of increasing removal of residual ligands such as C from the clusters with increasing severity of treatment in H_2. Other possibilities include a steric effect of the support, limiting adsorption of the reactants on the metal—such an effect would be greatest for the smallest clusters. Electronic effects should not be ruled out.

The result that the catalytic activities of extremely small clusters are different from those of larger nanoclusters and nanoparticles, even for structure-insensitive reactions, is broadly borne out by the work of Heiz and Colleagues (1999) for catalysts made by deposition of size-selected gas-phase clusters. The results are qualitatively consistent with results showing unique reactivities of gas-phase clusters (for example, Schnabel and Irion (1992) observed that Fe_n^+ clusters ($4 \leq n \leq 13$) are unreactive for bonding and dehydrogenation of ethane, except for $n = 4$ or 5), although these results cannot be extrapolated easily to supported clusters because the support exerts a strong influence on the reactivity. Much work remains to be done to connect the chemistry of metal complexes and clusters on supports with that of metal atoms and clusters in the gas phase (Armentrout, 1999), and research with well-defined supported metal complexes and nanoclusters should help forge the link.

The supported nanoclusters described above have strong connections to industrial catalysts, although the nanoclusters in industrial catalysts are much less uniform and less susceptible to incisive structural characterization than the materials considered here. Clusters of only a few metal atoms are applied in technology, e.g., Pt clusters in zeolite LTL for alkane dehydrocyclization (Jentoft *et al.,* 1998; Vaarkamp *et al.,* 1993; Miller *et al.,* 1993). EXAFS and transmission electron microscopy indicate Pt clusters containing from 5 to 12 atoms each, on average (Jentoft *et al.,* 1998; Vaarkamp *et al.,* 1993; Miller *et al.,* 1993). PdPt clusters of approximately this size are also present in new zeolite-supported catalysts for aromatic hydroprocessing in the presence of sulfur to meet stringent new fuel quality specifications; the extremely small clusters are resistant to poisoning by sulfur (Yasuda, Sato, and Yoshimura, 1999; Baird *et al.,* 1997). Furthermore, two- and three-atom clusters of Pt on γ-Al_2O_3 (Pt/γ-Al_2O_3) were observed, along with larger Pt nanoclusters, in conventionally prepared Pt/γ-Al_2O_3 by scanning transmission electron microscopy (Nellest and Pennycook, 1996). The roles of extremely small (and possibly undetected) clusters in many practical catalysts remain to be determined; for example, they could be important in supported gold catalysts, the remarkable catalytic properties of which are not yet well understood (Haruta, 1997).

E. GENERALIZATIONS ABOUT STRUCTURE, BONDING, REACTIVITY, AND CATALYSIS

The results just summarized lead to the following generalizations about supported metal nanoclusters:

- There is good agreement between EXAFS data and theoretical results characterizing structure and bonding in supported metal nanoclusters and the metal–support interface.
- The results indicate bonding interactions between the clusters and oxygen atoms of the supports; the supports are regarded as polydentate ligands for the clusters, much as they are ligands for metal complexes.
- Theory indicates that supported nanoclusters typified by Ir_4 on zeolite NaX are nearly neutral.
- Theory indicates that supported nanoclusters typified by Os_5C on MgO are bonded more strongly at surface defect sites than at defect-free sites.
- Supported clusters of only a few metal atoms have new catalytic properties, different from those of larger supported nanoclusters and nanoparticles.

V. Supported Metal Nanoparticles

Most supported metal catalysts incorporate metals in nanoclusters or nanoparticles larger than those considered above. A typical nanoparticle diameter is in the range 1 to 10 nm. Metal particles in this size range are usually large enough to have bulklike properties, and it is common to refer to them as metallic. They may expose various crystal faces, which may have different catalytic activities. Catalytic properties of nanoparticles, especially those with diameters in the approximate range 1 to 5 nm, may depend strongly on the particle sizes and shapes—and their interactions with the support, which influence the size and shape—at least in part because these influence the distribution of crystal faces that are exposed (Boudart, 1985). Nanoparticles with diameters greater than about 5 nm may have fully developed crystallographic habits, so that the particle size barely affects the catalytic activity.

The properties of nanoparticles may often be significantly different from those of the smaller nanoclusters discussed above, which may have unique catalytic sites, different from those on nanoparticles (Argo and Gates, forthcoming).

ACKNOWLEDGMENTS

This work was supported by the Department of Energy, Office of Energy Research, Office of Basic Energy Sciences, a gift from Ford Motor Co., and the National Science Foundation (Grant CTS-9615257).

REFERENCES

Alexeev, O., and Gates, B. C., EXAFS characterization of supported metal-complex and metal-cluster catalysts made from organometallic precursors, *Top. Catal.* **10,** 273 (2000).

Armentrout, P. B., Gas phase organometallic chemistry, *in* "Topics in Organometallic Chemistry" (J. M. Brown and P. Hofmann, Eds.), Vol. 4, p. 1. Springer Verlag, Berlin, 1999.

Baird, W. C. Jr., McVicker, G. B., Schorfheide, J. J., Klein, D. P., Hantzer, S., Daage, M., Touvelle, M. S., Ellis, E. S., Vaughan, D. E. W., and Chen, J. G., U.S. Patent 5935420 (1997).

Basset, J.-M., Lefebvre, F., and Santini, C., Surface organometallic chemistry: Some fundamental features including the coordination effects of the support. *Coord. Chem. Rev.* **180,** 1703, (1998).

Boudart, M., Heterogeneous catalysis by metals. *J. Mol. Catal.* **30,** 27 (1985).

Boudart, M., and Djéga-Mariadassou, G., "Kinetics of Heterogeneous Catalytic Reactions." Princeton University Press, Princeton, 1984.

Brenner, A., Comparative catalytic activity of supported clusters, *in* "Metal Clusters" (M. Moskovits, Ed.), p. 249. Wiley-Interscience, New York, 1986.

Budge, J. R., Scott, J. P., and Gates, B. C., Synthesis and characterization of an alumina-supported $RuOs_3$ cluster catalyst. *J. Chem. Soc., Chem. Commun.* **1983,** 342 (1983).

Che, M., From unit operations to elementary processes: A molecular and multidisciplinary approach to catalyst preparation. *Stud. Surf. Sci. Catal.* **130,** 115 (2000).

Che, M., Clause, O., and Marcilly, C., Supported catalysts. Deposition of active component. Impregnation and ion exchange, *in* "Preparation of Solid Catalysts" (G. Ertl, H. Knözinger, and J. Weitkamp, Eds.), p. 315 Wiley-VCH, Weinheim, 1999.

Deutsch, S. E., Chang, J.-R., and Gates, B. C., Osmium subcarbonyls on γ-alumina: Characterization of the metal-support bonding by infrared, nuclear magnetic resonance, and X-ray absorption spectroscopies. *Langmuir* **9,** 1284 (1993).

Dossi, C., Psaro, R., Roberto, D., Ugo, R., and Zanderighi, G. M., Surface-mediated synthesis of $H_4Ru_4(CO)_{12}$, $H_4Os_4(CO)_{12}$ on hydroxylated silica. *Inorg. Chem.* **29,** 4368 (1990).

Ferrari, A. M., Neyman, K. M., Mayer, M., Staufer, M., Gates, B. C., and Rösch, N., Faujasite-supported Ir_4 clusters: A density functional model study of metal–zeolite interactions. *J. Phys. Chem. B* **103,** 5311 (1999).

Gates, B. C., Surface-mediated synthesis of metal clusters. *J. Mol. Catal.* **86,** 95 (1994).

Gates, B. C., Supported metal clusters: Synthesis, structure, and catalysis. *Chem. Rev.* **95,** 511–522 (1995).

Gates, B. C., Metal cluster catalysts dispersed on solid supports, *in* "Catalysis by Di- and Polynuclear Metal Cluster Complexes" (R. D. Adams and F. A. Cotton, Eds.), p. 509. Wiley-VCH, New York, 1998.

Gates, B. C., Guczi, L., and Knözinger, H., (Eds.), "Metal Clusters in Catalysis." Elsevier, Amsterdam, 1986.

Gates, B. C., and Lamb, H. H., Supported metals and supported organometallics, *J. Mol. Catal.* **52,** 1 (1989).

Goellner, J. P, and Gates, B. C., Synthesis and characterization of site-isolated hexarhodium clusters on titania powder. *J. Phys. Chem. B.* **105,** 3269 (2001).

Goellner, J. F., Gates, B. C., Vayssilov, G., and Rösch, N., Structure and bonding of a site-isolated transition metal complex: Rhodium dicarbonyl in highly dealuminated zeolite Y. *J. Am. Chem. Soc.* **122,** 8056 (2000).

Goellner, J. F., Neyman, K. M., Mayer, M., Nörtemann, F., Gates, B. C., and Rösch, N., Ligand-free osmium clusters supported on MgO. A density functional study. *Langmuir* **16,** 2736 (2000).

Haruta, M., Size-and support-dependency in the catalysis of gold. *Catal. Today* **36,** 153 (1997).

Heiz, U., Sanchez, A., Abbet, S., and Schneider, W.-D., Catalytic oxidation of carbon monoxide on monodispersed platinum clusters: Each atom counts. *J. Am. Chem. Soc.* **121,** 3214 (1999).

Heiz, U., and Schneider, W.-D., Nanoassembled model catalysts. *J. Phys. D—Appl. Phys.* **33,** R85 (2000).

Hu, A., Neyman, K. M., Staufer, M., Belling, T., Gates, B. C., and Rösch, N., A surface site as polydentate ligand of a metal complex: Density functional studies of rhenium subcarbonyls supported on magnesium oxide. *J. Am. Chem. Soc.* **121,** 4522 (1999).

Ichikawa, M., Metal cluster compounds as molecular precursors for tailored metal catalysts. *Adv. Catal.* **38,** 283 (1992).

Iwasawa, Y., Chemical design surfaces for active solid catalysts. *Adv. Catal.* **35,** 187 (1987).

Iwasawa, Y., Chemical design and characterization of catalysts and catalysis—an approach to dynamic catalyst design. *Catal. Today* **18,** 21–72 (1993).

Jentoft, R. E., Tsapatsis, M. A., Davis, M. E., and Gates, B. C., Platinum clusters supported in zeolite LTL: Influence of catalyst morphology on performance in *n*-hexane reforming. *J. Catal.* **179,** 565 (1998).

Kaminsky, W., Metallocene catalysts for olefin polymerization, *in* "Science and Technology in Catalysis 1998" (V. Dragutan and R. Streck, Eds.), p. 3. Elsevier, Amsterdam, 1999.

Kawi, S., Chang, J.-R., and Gates, B. C., Tetrairidium clusters supported on γ-Al_2O_3: Formation from $[Ir_4(CO)_{12}]$ and CO-induced morphology changes. *J. Phys. Chem.* **97,** 5375 (1993).

Kawi, S., and Gates, B. C., Clusters in cages, *in* "Clusters and Colloids" (G. Schmid, Ed.), p. 299. VCH, Weinheim, 1994.

Kirlin, P. S., DeThomas, F. A., Bailey, J. W., Gold, H. S., Dybowski, C., and Gates, B. C., Molecular oxide-supported rhenium carbonyl complexes: Synthesis and characterization by vibrational spectroscopy. *J. Phys. Chem.* **90,** 4882 (1986).

Kirlin, P. S., and Gates, B. C., Activation of the C–C bond provides a molecular basis for structure sensitivity in catalysis. *Nature* (*London*) **325,** 38 (1987).

Kirlin, P. S., Knözinger, H., and Gates, B. C., Mononuclear, trinuclear, and metallic rhenium catalysts supported on MgO: Effects of structure on catalyst performance. *J. Phys. Chem.* **94,** 8451 (1990).

Kirlin, P. S., van Zon, F. B. M., Koningsberger, D. C., and Gates, B. C., Surface catalytic sites prepared from $[HRe(CO)_5]$ and $[H_3Re_3(CO)_{12}]$: Mononuclear, trinuclear, and metallic rhenium catalysts supported on MgO. *J. Phys. Chem.* **94,** 8439 (1990).

Koningsberger, D. C., and Gates, B. C., Nature of the metal–support interface in supported metal catalysts: Results from X-ray absorption spectroscopy. *Catal. Lett.* **14,** 271 (1992).

Kristen, M. O., Supported metallocene catalysts with MAO and boron activators. *Top. Catal.* **7,** 89 (1999).

Lamb, H. H., Gates, B. C., and Knözinger, H., Molecular organometallic chemistry on surfaces: Reactivity of metal carbonyls on metal oxides. *Angew. Chem. Int. Ed. Engl.* **27,** 1127 (1988).

Li, X.-J., Gates, B. C., Knözinger, H., and Alizo Delgado, E., Support effects in hexene-1 isomerization catalyzed by oxide-supported osmium complexes. *J. Catal.* **88,** 355 (1984).

Meiwes-Broer, K.-H., (Ed.), "Metal Clusters at Surfaces." Springer, Heidelberg, 2000.

Messerli, S., Schintke, S., Morgenstern, K., Sanchez, A., Heiz, U., and Schneider, W.-D., Imaging size-selected silicon clusters with a low-temperature scanning tunneling microscope. *Surf. Sci.* **465,** 331 (2000).

Miessner, H., Surface-chemistry in a zeolite matrix—Well-defined dinitrogen complexes of rhodium supported on dealuminated Y-zeolite. *J. Am. Chem. Soc.* **116,** 11522 (1994).

Miessner, H., Burkhardt, I., Gutschick, D., Zecchina, A., Morterra, C., and Spoto, G., The formation of a well-defined rhodium dicarbonyl in highly dealuminated rhodium-exchanged zeolite-Y by interaction with CO. *J. Chem. Soc., Faraday Trans. I* **85,** 2113 (1989).

Miller, J. T., Meyers, B. L., Modica, F. S., Lane, G. S., Vaarkamp, M., and Koningsberger, D. C., Hydrogen temperature-programmed desorption (H_2 TPD) of supported platinum catalysts. *J. Catal.* **143,** 395 (1993).

Nellist, P. D., and Pennycook, S. J., Direct imaging of the atomic configuration of ultradispersed catalysts. *Science* **274,** 413 (1996).

Panjabi, G., Argo, A. M., and Gates, B. C., Supported iridium cluster catalysts for propene hydrogenation: Identification by X-ray absorption spectra measured during catalysis. *Chem. Eur. J.* **5,** 2417 (1999).

Panjabi, G. A., Salvi, S. N., Phillips, B. L., Allard, L. F., and Gates, B. C., Ph.D. Thesis, University of California, Davis (2000).

Papile, C. J., and Gates, B. C., Rhenium subcarbonyls on magnesium oxide: Identification of the surface oxo and hydroxo ligands by infrared spectroscopy. *Langmuir* **8,** 74 (1992).

Purnell, S. K., Xu, X., Goodman, D. W., and Gates, B. C., Adsorption and reaction of $[Re_2(CO)_{10}]$ on ultrathin MgO films grown on a Mo(110) surface: Characterization by infrared reflection–absorption spectroscopy and temperature-programmed desorption. *J. Phys. Chem.* **98,** 4076 (1994a).

Purnell, S. K., Xu, X., Goodman, D. W., and Gates, B. C., Adsorption and reaction of $[HRe(CO)_5]$ on ultrathin MgO(111) and amorphous SiO_2 films grown on a Mo(110) Surface: Characterization by infrared reflection–absorption spectroscopy and temperature-programmed desorption. *Langmuir* **10,** 3057 (1994b).

Roberto, D., Cariati, E., Ugo, R., and Psaro, R., Surface-mediated organometallic synthesis: High-yield preparations of neutral and anionic osmium carbonyl clusters by controlled reduction of silica-supported $[Os(CO)_3Cl_2]_2$ and $OsCl_3$ in the presence of Na_2CO_3 or K_2CO_3. *Inorg. Chem.* **35,** 2311 (1996).

Roscoe, S. B., Frechet, J. M. J., Walzer, J. F., and Dias, A. J., Polyolefin spheres from metallocenes supported on noninteracting polystyrene. *Science* **280,** 270 (1998).

Schnabel, P., and Irion, M. F., Reactions of $Fe_n^+(3 \leq n \leq 12)$ with ethane, ethylene and acetylene—reaction paths and rate constants. *Ber. Bunsenges. Phys. Chem.* **96,** 1101 (1992).

Sullivan, D. L., Roark, R. D., Ekerdt, J. G., Deutsch, S. E., and Gates, B. C., Reaction and spectroscopic study of silica-supported molybdenum(IV) and tungsten(IV) dimers. *J. Phys. Chem.* **99,** 3678 (1995).

Triantafillou, N. D., and Gates, B. C., Magnesia-supported tetrairidium clusters derived from $[Ir_4(CO)_{12}]$. *J. Phys. Chem.* **98,** 8431 (1994).

Triantafillou, N. D., Purnell, S. K., Papile, C. J., Chang, J.-R., and Gates, B. C., A Family of rhenium subcarbonyls on MgO: Structural characterization by extended X-ray absorption fine structure spectroscopy. *Langmuir* **10,** 4077 (1994).

Vaarkamp, M., Modica, F. S., Miller, J. T., and Koningsberger, D. C., Influence of hydrogen pretreatment on the structure of the metal–support interface in Pt/zeolite catalysts. *J. Catal.* **144,** 611 (1993).

van Zon, F. B. M., Maloney, S. D., Gates, B. C., and Koningsberger, D. C., Structure and nature of the metal–support interface: Characterization of iridium clusters on magnesium oxide by extended X-ray absorption fine structure spectroscopy. *J. Am. Chem. Soc.* **115,** 10317 (1993).

van't Blik, H. F. J., van Zon, J. B. A. D., Huizinga, T., Vis, J. C., Koningsberger, D. C., and Prins, R., Structure of rhodium in an ultradispersed Rh/Al_2O_3 catalyst as studied by EXAFS and other techniques. *J. Am. Chem. Soc.* **107,** 3139 (1985).

Vidal, V., Theolier, A., Thivolle Cazat, J., and Basset, J.-M., Metathesis of alkanes catalyzed by silica-supported transition metal hydrides. *Science* **276,** 99 (1997).

Wovchko, E. A., and Yates, J. T., Chemical bond activation on surface sites generated photochemically from $Rh(I)(CO)_2$ species. *Langmuir* **15,** 3506 (1999).

Xiao, F.-S., Weber, W. A., Alexeev, O., and Gates, B. C., Probing the limits of structure insensitivity: Size-dependent catalytic activity of Al_2O_3-supported iridium clusters and particles for toluene hydrogenation. *Stud Surf. Sci. Catal.* **101,** 1135 (1996).

Xu, Z., Xiao, F.-S., Purnell, S. K., Alexeev, O., Kawi, S., Deutsch, S. E., and Gates, B. C., Size-dependent catalytic activity of supported metal clusters. *Nature* (*London*) **372,** 346 (1994).

Yasuda, H., Sato, T., and Yoshimura, Y., Influence of the acidity of USY zeolite on the sulfur tolerance of Pd-Pt catalysts for aromatic hydrogenation. *Catal. Today* **50,** 63 (1999).

Zhao, A., and Gates, B. C., Probing metal oxide surface reactivity with adsorbate organometallic chemistry: Formation of iridium carbonyl clusters on γ-Al_2O_3, *Langmuir* **13,** 4024 (1997).